Catena 207 (2021) 105621

Contents lists available at ScienceDirect

Catena

journal homepage: www.elsevier.com/locate/catena

Characteristics and prevention mechanisms of artificial slope instability in the Chinese Loess Plateau

Xuanchang Zhang [a,c], Yurui Li [a,b,*], Yansui Liu [a,b,c,*], Yunxin Huang [a,c], Yongsheng Wang [a,b], Zhi Lu [d]

[a] Institute of Geographic Sciences and Natural Resources Research, Chinese Academy of Sciences, Beijing 100101, China
[b] Key Laboratory of Regional Sustainable Development Modeling, Chinese Academy of Sciences, Beijing 100101, China
[c] University of Chinese Academy of Sciences, Beijing 100049, China
[d] Peter B. Gustavson School of Business, University of Victoria, BC V8P5C2, Canada

ARTICLE INFO

Keywords:
Artificial slope instability
Gully Land Consolidation project
Back Propagation Neural Network (BPNN)
Gutun watershed

ABSTRACT

Numerous artificial slopes emerged in the watersheds of the Chinese Loess Plateau (LP) after the Gully Land Consolidation project (GLCP) that cut slopes to create farmland in the gully, which had incurred instabilities over time and could potentially resulted in soil erosion and geological hazard. This paper explored the characteristics and prevention mechanisms of artificial slope instability after the GLCP with field investigation in a typical watershed and the Back Propagation Neural Network (BPNN) method. The results showed that: (1) 439 instabilities induced by infiltration and erosion were found in 79 artificial slopes. (2) The difference of soil moisture and failure mode resulted in the instability degree of shady slope and lower slope were significantly higher than that of sunny slope and upper slope. (3) Among the surface condition factors, slope instability volume was significantly influenced by gradient, soil compactness, height and soil shear strength. Platform instability volume had great connection with soil compactness and its shear strength. (4) A "Drain-Improve-Green-Reinforce (DIGR)" system was proposed as the prevention mechanism for artificial slope instability, which included drainage system, soil improvement, vegetation protection, and reinforcement engineering. Taken together, this research provides the scientific reference for a better understanding and prevention of artificial slope instability, which would contribute to ensuring GLCP effectiveness and ecological security in the LP.

1. Introduction

Every year many geological disasters caused by slope instabilities, such as landslide, collapse, and debris flow, pose a serious threat to ecological security and human safety all over the world (Guzzetti et al., 1999; Gomez and Kavzoglu, 2005; Lukić et al., 2018; Peng et al., 2019; Tan et al., 2021). With the intensification of human activities, there is an obvious trend that many geological disasters that are caused by slope instabilities are related to human's engineering works (Sutejo and Gofar, 2015; Peng et al., 2016; Ai et al., 2019). Numerous artificial slopes have been inevitably produced by the cut-slopes in the infrastructure construction, mine exploitation and land consolidation, especially in the mountainous and hilly regions (Rupke et al., 2007; Liu and Li, 2017; Levett et al., 2020). During the process, soil properties of artificial slopes are degraded given the topsoil and vegetation were destroyed in comparison with the natural slopes. It is difficult to restore by solely relying on natural forces over a short-term period (Mota et al., 2004; Lee et al., 2013; Chen et al., 2016). In addition, artificial slopes are susceptible to damage from external forces which are very likely lead to slope instabilities, especially for steeper slopes. These slope instabilitieshave severe impact on the sustainable development of social-ecological system (Lee et al., 2009; Ai et al., 2019).

Many studies had conducted on the artificial slope instability to reduce the risk of geological hazards with the increasing number of these slopes. Some studies assessed the stability of artificial slopes in different regions through the remote sensing, field monitoring and experimental simulation (Jia et al., 2015; Shin et al., 2020), and discussed the influence of it on regional sustainable development (Sutejo and Gofar, 2015). The soil physic-chemical properties and structural characteristics of artificial slope were studied using rising shear and triaxial tests methods

* Corresponding authors at: Chinese Academy of Sciences, Institute of Geographic Sciences and Natural Resources Research, 11A Datun Road, Chaoyang District, Beijing, 100101, China.
E-mail addresses: liyr@igsnrr.ac.cn (Y. Li), liuys@igsnrr.ac.cn (Y. Liu).

https://doi.org/10.1016/j.catena.2021.105621
Received 12 April 2021; Received in revised form 17 July 2021; Accepted 23 July 2021
Available online 26 August 2021

(Chen et al., 2016; Ai et al., 2019; Ai et al., 2021). Several methods have been applied to identify the critical factors of artificial slope instability, such as the fuzzy set method, self-organization feature map and artificial neural network (Lee et al., 2009; Erzin and Cetin, 2012; Erzin et al., 2016). The development process of slope instability was investigated through field investigation and in-situ test (Crozier, 1999; Cho and Lee, 2001; Liang et al., 2018). For example, Peng et al. (2016) divided the landslide process triggered by engineering unloading into four stages: creep deformation, slip deformation, fissure propagation, and landslide instability. Meanwhile, extant research discussed the matters needing attention in the process of artificial slope construction based on the analysis of typical cases (Rupke et al., 2007). Many prevention measures of artificial slope instability were proposed based on the physical test, field monitoring, and engineering demonstration, such as geometry changes, engineering reinforcement, solidifying agent application and vegetation restoration (Xu et al., 2012; Zhao et al., 2018; Feng et al., 2019; Levett et al., 2020). Existing research mainly focused on the instability of artificial slope created by the highway or railway construction. However, the instability characteristics and mechanisms of artificial slopes are significantly different across various regions and engineering types. It is necessary to carry out an in-depth study on the instability of artificial slopes induced by typical engineering in special region.

The loess area is plagued by the geological disasters caused by slope instability due to the loess characteristics of vertical joints, loose texture, higher collapsibility, and water sensitivity (Zhang and Liu, 2010; Zhuang et al., 2018; Feng et al., 2021). Chinese Loess Plateau (LP) is one of the regions with the most widely distributed loess in the world. The LP develops many slope instabilities which lead to geological hazards every year, and has shown an increasing tendency with the intensity of human activities in recent year (Tu et al., 2009; Peng et al., 2018; Li et al., 2021). Statistical data reveals that up to 11,768 geological hazards relating to slope instability occurred in Shaanxi Province of the LP in 2017. Since 2012, the LP implemented the Gully Land Consolidation project (GLCP) in 197 watersheds to alleviate the farmland shortage after the Grain-for-Green project (Chen et al., 2015; Jin et al., 2019; Liu and Wang, 2019). The GLCP effectively improved the farmland quantity, while many steep artificial slopes emerged because the GLCP applied the method of cut slopes and fill gully filled to create farmland (Jin, 2014; Li et al., 2019; Liu et al., 2020). Some measures have been adopted to enhance the stability of artificial slopes (Liu and Li, 2017), but many instabilities were still found in the recent field investigation (Feng and Li, 2021). The instabilities of artificial slopes might lead to serious soil erosion, block gully channel and bury newly created farmland. Hence, it is important to study the characteristics and prevention mechanism of artificial slope instability after the GLCP to ensure the project effectiveness and ecological security.

In view of this, this study took the Gutun watershed as case study area and focused on the instability of artificial slopes after the GLCP in the LP. We applied the field investigation and Back Propagation Neural Network (BPNN) to an in-depth analysis in this research. Specifically, this paper aims to: a) identify the characteristics and spatial distribution of the artificial slope instability; b) analyze the influencing extents of slope surface condition factors on the instability volume; c) explore the prevention mechanism of the artificial slope instability.

2. Materials and methods

2.1. Study area

The study area is located in the Gutun watershed (36°45′-36°50′N, 109°46′-109°51′E), Baota District, Yan'an City of Shaanxi Province, China. Gutun is a typical watershed in the loess hilly-gully region of the LP. The length and total area of Gutun watershed are 12.50 km and 24.87 km^2 respectively (Fig. 1). There are ravines, ridges, deep valleys, and tattered landforms in this watershed, composed of three

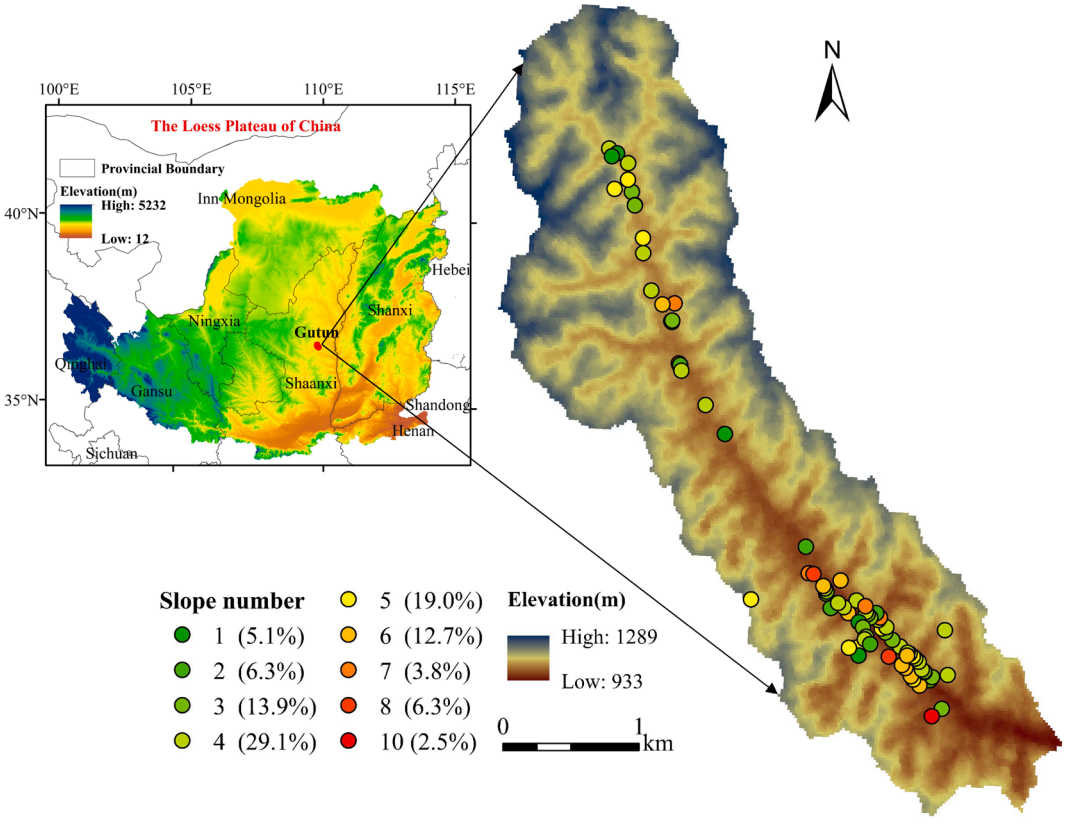

Fig. 1. Location of the Gutun watershed in the LP and the investigated artificial slopes: slope number indicates the number of layers on a slope.

geomorphologies, including ridges, gully slopes, and gully bed. The elevation of this watershed is between 933 and 1289 m titling from southeast to northwest. The direction of main gully result in most slopes orienting west or east. The watershed is covered with quaternary loess, including Malan loess, Heilu soil and Red clay. Climate in the study area comprises a semi-arid monsoon climate with an annual average temperature of 9.80 °C and a precipitation of 541 mm. The summer precipitation accounts for about 50–70% of the annual precipitation and is often accompanied by high-intensity thunderstorms (Wang et al., 2019). The GLCP has been implemented since 2013 in the Gutun watershed, which created 159.06 hm^2 new farmland in the gully. Many artificial slopes produced in both sides of the gully in the process of cutting slopes and filling gullies (Li et al., 2019). The vegetation coverage of artificial slopes is relatively lower compared to that of natural slopes, and shows significant differences across different slopes. The dominant species of vegetation in the artificial slopes are *Robinia* (Linn.), *Caragana korshinskii* (Kom.), *Hippophae* (Linn.) and *Stipa bungeana* (Trin.).

2.2. Investigation design and data collection

According to the characteristics of artificial slope after the GLCP, the study designed an investigated method of artificial slope instability. The investigation contents include the following aspects. **1) Slope situation.** The longitude, latitude, elevation, relative height, slope's aspect and layer were recorded with the help of Hand GPS (G120BD). **2) Surface condition.** The slope's gradient, length and height, platform's width, vegetation and soil physical property of each layer were measured on the spot. The Laster rangefinder (XR-1800C) was used to measure the gradient and length in the slope middle and sides. The gradient, length and height of each slope were then obtained by calculating the average values and trigonometry value. The same method was used to measure the width of each platform. Three repeated quadrats (area: 2 × 2 m) were set up to observe the vegetation types, coverage and species in each slope and platform. The soil compactness of different depths (Slope: 0 and 10 cm; Platform: 0, 10, and 20 cm) and the shear strength of surface soil at five different points were determined by the Soil Compactor (SC-900) and the Soil Shear Tester (H-4212MH) in each quadrat along with an "S" pattern. The average values were calculated to obtain soil compactness and shear strength of each quadrat. **3) Instability characteristics.** The number of various instabilities were recorded in each slope and platform and their length, width (diameter), depth (thickness), soil compactness, and soil shear strength were measured. For the instability with an irregular shape, we adopted the piecewise method to determine segment volumes and added them to calculate total volume. The field investigation was conducted in July and August 2019 based on the above investigation method, and 79 artificial slopes were investigated in the Gutun watershed (Fig. 1). The 4-layers slope was the highest investigated frequency ratio (29.1%), the following was 5 (19.0%), 3 (13.9%), 6 (12.7%), 2 and 8 (6.3%), 1 (5.1%), 7 (3.8%) and 10 (2.5%) layers.

2.3. Data analysis

Analyzing the characteristics of artificial slope instability: Based on the field investigation data in the Gutun watershed, the basic features of artificial slope after GLCP were summarized, including the shape, layer, gradient, soil properties and vegetation of slope. The occurrence frequency and geometric features of various instabilities were analyzed to describe the characteristics of artificial slope instability. The slope aspect was divided into eight orientations according to the principle of equidistance. The frequency ratio and average volume of instabilities in the different slope aspects were counted to analyze the spatial distribution of the instabilities. The vertical distribution of the instabilities was discussed by the statistics of categories and average volumes in each layer slope and platform.

Analyzing the factors influencing artificial slopes instability: Artificial slope instability is the nonlinear interaction result of surface condition factors. In addition, the influence of different factors is uncertain (Rupke et al., 2007). In order to precisely estimate the influencing degree of various factors on the instability, this study applied the Back Propagation Neural Network (BPNN) method to construct a simulation model. The BPNN is a multilayer feed-forward network including input layer, hidden layer, and output layer (Fig. 2), which has strong knowledge acquisition ability and nonlinear mapping function. This method is getting increasingly more attention in the analysis of slope stability because it could approach any nonlinear function by the arbitrary precision (Gomez and Kavzoglu, 2005; Suman et al., 2016).

This study used the *SPSS* 22.0 statistical software to construct the BPNN of slope and platform for instability simulation, respectively. The total volume of instability in each slope and platform was taken as dependent variable, and it would set as 0 if no instability occurred in the slope and platform. The key factors were selected as independent variables from the perspectives of topography, geological condition, and surface coverage. The topography obviously determines whether the slope has the precondition of instability. The slope aspect, the gradient and height of slope and platform width affect the slope stability by changing the gravity action and runoff collection (Qiu et al., 2017; Peng et al., 2018). The geological condition and surface coverage significantly impact on the properties of surface and deep soil. The weaker soil might be more prone to instability, while vegetation coverage would enhance the soil stability to make the slope stable (Chen et al., 2016). Therefore, slope gradient, aspect and height, soil compaction-0/10 cm, and soil shear strength, arbor/shrub/grass/moss coverage were regarded as independent variables of slope instability. Platform aspect and width, soil compaction-0/10/20 cm and soil shear strength, arbor/shrub/grass coverage are independent variables of platform instability.

Investigated sample P was normalized by the variance standardization method, which was randomly set as training and inspection sample in the proportion of 8:2. Subsequently, the Levenberg-Marquardt algorithm was adopted to train BPNN parameters, and the minimum mean square error determined the optimal BPNN. To validate the accuracy of the BPNN, this study used the root mean square error (*RMSE*) and correlation coefficient (R^2) to quantitatively describe the errors between fitted and measured values. The *RMSE* and R^2 were calculated by Eqs. (1) and (2), respectively. Based on the optimal BPNN, we calculated the mean impact values (MIV) of each surface condition factor to estimate its influencing degree. The absolute value of the MIV measured the influencing degree on the volume of instability, and the MIV direction indicated the positive or negative effect. MIV calculation includes the following four steps: 1) Factor change. New samples P_1 and P_2 being formed by adding or subtracting 10% of a factor keeping the other factors constant in the sample P; 2) BPNN simulation. New samples P_1 and P_2 were inputted into the optimal BPNN to obtain the results A_1 and A_2 respectively; 3) MIV calculation. The MIV of this factor was obtained by the mean value of the difference between A_1 and A_2, and the MIV of other factors were obtained by repeating the previous steps.

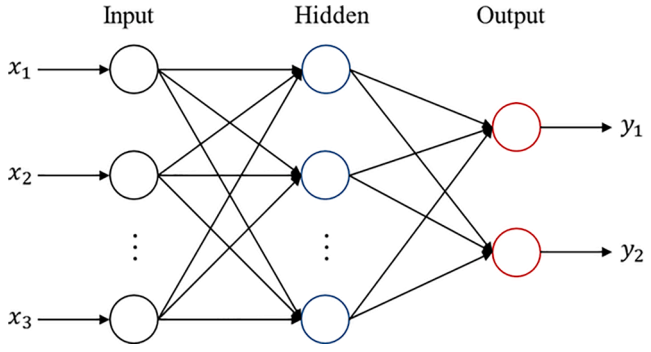

Fig. 2. The framework of Back Propagation Neural Network.

$$RMSE = \sqrt{\frac{\sum_{i=1}^{n}\left(\widehat{y}_i - y_i\right)^2}{n}} \quad (1)$$

$$R^2 = \frac{\sum_{i=1}^{n}\left(\widehat{y}_i - \overline{y}\right)^2}{\sum_{i=1}^{n}\left(y_i - \overline{y}\right)^2} \quad (2)$$

where $\widehat{y}_i$, y_i and $\overline{y}$ are the instability of fitted, measured and average value respectively, n is the sample number.

3. Results

3.1. Basic features of artificial slope

The artificial slopes created by the GLCP are mainly stepped structures distributing along the gully (Fig. 3). The top of the artificial slope is connected with the natural slope, and the toe of the slope is close to the gully or road. The relative height of the artificial slope is 15–80 m and the number of layers primarily is 4–5 with the maximum number being up to 10. Each slope gradient is almost more than 60° that gradually decreases from top to toe, while slope height and platform width gradually increase. Taking the 4-layers slope as an example, the average gradient of each slope is 77.4°, 72.9°, 69.6°, and 67.3° from top-slope to toe-slope, and the slope height and platform width increases from 595.0 and 256.5 cm to 661.9 and 324.8 cm, respectively. The soil types of artificial slope present layered distribution. The upper, middle, and lower slope are Malan loess, Lishi loess, and Wucheng loess, respectively. The paleosol exists between different loess types, and the rock distributes in the toe of slope. The average soil shear strength, soil compactness-0 cm and −10 cm of slopes are 5.4 kg cm^{-2}, 361.1 Pa, and 677.1 Pa, respectively. The average soil shear strength, soil compactness-0 cm, −10 cm and −20 cm of platforms are 5.1 kg cm^{-2}, 363.6 Pa, 829.4 Pa, and 1210.6 Pa, respectively. The vegetation coverage of artificial slope is relatively lower than that of natural slope. The dominant vegetation in the slope is moss, and the vegetation coverage in the platform are mainly the combination of arbor, shrub and grass which has no significant difference among different platforms.

3.2. Instability characteristics of artificial slope

The field investigation founded 439 instabilities in 79 artificial slopes, of which 328 were in the slope and 121 were in the platform (Table 1). The erosion gully, sinkhole, landslide, collapse and slump were the main categories of slope instability, accounting for 41.5%, 11.7%, 14.6%, 23.1%, and 9.2% of total instabilities in the slopes, respectively. Most of the erosion gullies were rills with an average volume of 2.3 m^3. The sinkholes were mostly distributed in the top or bottom of the erosion gully with an average volume of 1.2 m^3. The size of landslides, collapses and slumps was relatively small. The landslides were mainly homogenous loess, retrogressive and shallow landslides with an average volume of 16.5 m^3. Most of the collapses were stripping collapses, and a few of them were subsiding collapses in the slope with a lager gradient and height. The slump size between landslide and collapse, and the average volume of which was 45.2 m^3. The categories of platform instabilities were ground subsidence and sinkhole, and the proportions of which were 65.0% and 35.0%. The ground subsidence showed the "Y" or "—" shape, while the size of which was significantly different. The minimum length, width, depth, and volume of ground subsidence were 19.6 cm, 14.2 cm, 13.0 cm, 0.1 m^3, but the maximum was up to 34.3 cm, 6.1 cm, 2.0 cm, and 47.6 m^3. The platform sinkhole was on average 84.5 cm in diameter and average 131.1 cm in depth with an average volume of about 1.5 m^3.

3.3. Instability distribution of artificial slope

Fig. 4 showed the variation in instabilities frequency and volume of the artificial slope with the slope aspect. The maximum frequency ratio and the average volume of slope instability occurred at the slopes orienting 45-90° (i.e., Northeast to East), which were 40.2% and 40.8 m^3 respectively. The frequency ratio of slope instability was the second in the slopes orienting 225-270° (i.e. Southwest to West), but the average

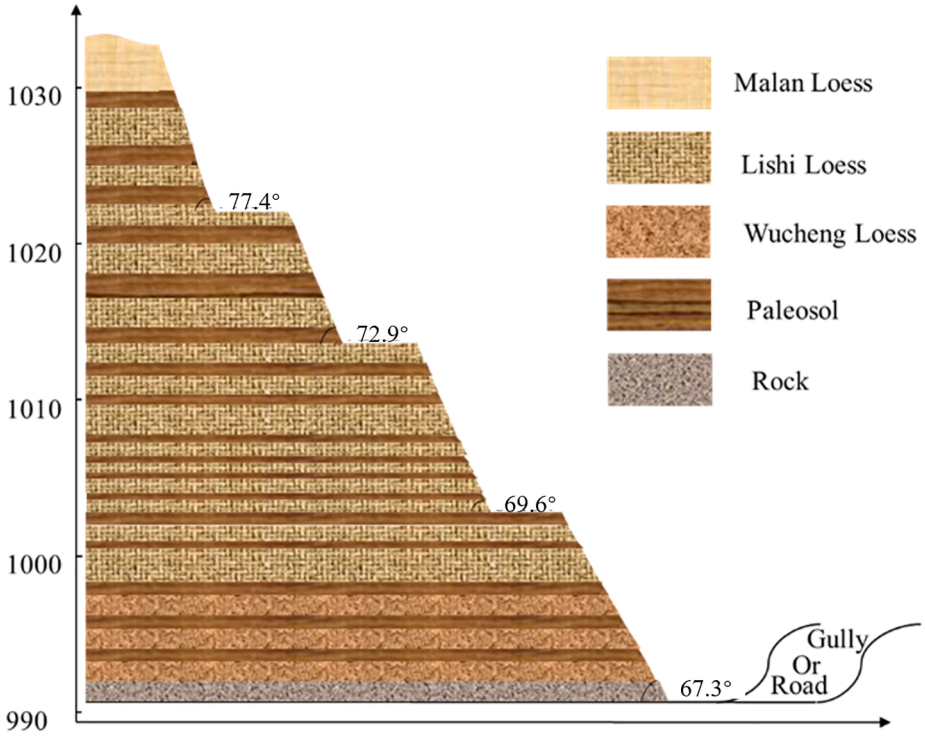

Fig. 3. The basic features of artificial slope (4-layers) in the Gutun watershed.

Table 1
The instability characteristics of artificial slope in the Gutun watershed.

		Frequency (%)	Length (cm)	Width/Diameter (cm)	Depth/Thickness (cm)	Volume (m^3)
Slope	Erosion gully	41.5	443.6 ± 174.0	45.5 ± 50.3	52.2 ± 45.2	2.3 ± 9.3
	Sinkhole	11.7	–	64.7 ± 38.2	149.1 ± 132.8	1.2 ± 2.6
	Landslide	14.6	538.1 ± 247.2	788.7 ± 592.3	33.2 ± 11.8	16.5 ± 15.4
	Collapse	23.1	510.4 ± 711.1	878.6 ± 780.7	91.3 ± 52.9	147.8 ± 460.1
	Slump	9.2	411.5 ± 173.7	999.9 ± 1079.2	59.0 ± 49.4	45.2 ± 92.5
Platform	Ground subsidence	65.0	347.8 ± 452.2	128.7 ± 159.6	78.5 ± 48.1	6.2 ± 13.7
	Sinkhole	35.0	–	84.5 ± 51.3	131.0 ± 116.5	1.5 ± 2.3

volume of which (22.8 m^3) was less than that in the slopes orienting 135-180° (i.e., Southeast to South). There was no obvious difference in the frequency ratio and average volume of slope instability among other slope aspects. The highest frequency ratios and average volumes of platform instabilities were also located in the slopes orienting 45-90° (55.0% and 3.0 m^3). The slopes orienting 225-270° had the next higher frequency ratio (20.0%) and average volume (2.0 m^3) of platform instabilities. The remainder platform instabilities scattered in the other slope aspects, and average volume was relatively small. Combining with the direction of the Gutun watershed, the instabilities variation with the slope aspects indicated the shady slopes were associated with a higher probability and size of instability than the sunny slopes.

The 4-layers slope was taken as an example to analyze the vertical distribution of artificial slope instability because it accounted for the highest ratio of the investigated slopes (Fig. 5). Statistical results showed that the frequency ratio, category, and size of slope instability existed obvious differences among different layer slopes. The frequency ratio of slope instability was 11.3%, 20.6%, 18.6%, 49.5% from slope 1 to slope 4, respectively. The main instability categories of each layer slope were as follows: slope 1 was the erosion gully and slump, slope 2 was the erosion gully and landslide, slope 3 was the erosion gully, collapse, and sinkhole, slope 4 was the erosion gully, collapse, sinkhole, and few landslides, respectively. The average volumes of the instability in the slope 4 was 4.5 m^3 (Erosion gully), 1.2 m^3 (Sinkhole), 47.9 m^3 (Collapse) and 21.2 m^3 (Landslide), which were significantly greater than those in other slopes. The instability size increased layer by layer from slope 1 to slope 4, as the corresponding average volume of erosion gully was 0.9, 0.5, 0.6, and 4.5 m^3. The instability in the platform 1, 2, 3 accounted for 17.4%, 52.2%, 30.4%, respectively. The ground subsidence and sinkhole were mainly distributed on the sides or front edges of the platform, and most of which were connected with the erosion gully and sinkhole of the slope. The size of platform instability also showed a rising trend along with the layers. The average volume of ground subsidence and sinkhole were 0.9 and 0.2 m^3 in the platform 1, which increased to 1.3 and 0.4 m^3 in the platform 2 and 7.4 and 3.3 m^3 in the platform 3, respectively.

3.4. Influencing degrees of surface condition factors

The optimal BPNN and its parameters of slope/platform instability were determined through many rounds of training. The mean square error of the BPNN of slope and platform instability were 3.67% and 2.56%, respectively. The *RMSE* and R^2 of fitted and measured values of slope instabilities' BPNN were 14.39 and 0.80, and that of platform instabilities' BPNN were 2.31 and 0.95 (Fig. 6). Above parameters indicated the BPNN could truly simulate the dynamic changes of the instability with multiple surface condition factors.

The MIV order of surface condition factors of slope instability were gradient > soil compactness-10 cm > height > soil shear strength > soil compactness-0 cm > aspect > grass/moss coverage > shrub converge > arbor coverage (Table 2). The gradient, height, aspect, and grass coverage of slope had a positive effect on its instabilities' volume, and the influencing degree of slope gradient (0.45) and height (0.12) were relatively larger. Other factors had a negative correlation with the volume of slope instability, and the influencing degrees of soil compactness-10 cm (-0.14) and soil shear strength (-0.11) were the largest among the factors. The MIV order of surface condition factors of platform instability were soil compactness-10 cm > soil compactness-0 cm > soil compactness-20 cm > soil shear strength > width > aspect > arbor/shrub coverage > grass coverage. The width (0.05), aspect (0.02), and grass coverage (0.01) of the platform had a negative impact on the volume of platform instability, but the influencing degrees of which were relatively smaller. The volume of platform instability was gradually decreasing with the increase of soil compactness-10 cm (−0.16), compactness-0 cm (−0.12), compactness-20 cm (−0.09), and shear strength (−0.06).

4. Discussion

4.1. Cumulative instability process induced by rainfall

Loess properties and poor drainage lead to the increasing risk of artificial slope instability with the infiltration and erosion of rainfall. The loose texture, higher collapsibility, and water sensitivity of loess easily cause collapse, sliding and other deformation when meeting water (Acharya et al., 2011; Garakani et al., 2015). Many research indicated that rainfall infiltration and erosion is the most active inducing factor for loess landslide (Derbyshire, 2001; Tang et al., 2015; Zhuang et al., 2018). It is widely known that well-arranged drainage facilities could reduce the rainfall infiltration and erosion of artificial slope, which contributes to decrease the risk of slope instability (Xu et al., 2012). However, the GLCP did not changed the loess prosperities, and it further broke the original stress equilibrium state with increased gradient, which provide conditions for cracks, joints, and fissures. Meanwhile, given drainage facilities were not fully implemented in the artificial slopes according to the design scheme (Liu and Li, 2017). Therefore, the ground subsidence were formed on the top of the slope and platform, and the rainfall infiltrated into the slope along with the cracks, joints and fissures. The slope surface was also subjected to high-intensity erosion. During the heavy rainfall or consecutive rainy days, some instabilities would occur in the artificial slope. The small instabilities would enlarge and develop into a landslide, collapse, and slump under the long-term physical, mechanical and chemical effects of the infiltration water (Peng et al., 2018). Hence, the infiltration and erosion of rainfall caused by poor drainage were the fundamental reason inducing artificial slope instability after the GLCP.

We propose that artificial slope instability was a long-term cumulative process consisting of three stages: creeping deformation, expanding deformation, and instability failure (Fig. 7). **1) Creeping deformation stage**. Steep gradient of the artificial slope sharply increased the stress at the toe of the slope and the traction at the top of the slope, and the tension zone and small tensile cracks would be formed at the top of the slope and platform when the traction is greater than the soil shear strength (Peng et al., 2016). Rainfall could not be drained timely due to poor drainage, and it would infiltrate along the tensile cracks and decrease the cohesion of loess which contributes to the forming of ground subsidence in the slope-top/platform (Tu et al., 2009; Zhuang et al., 2018). Meanwhile, runoff erosion and rainfall splash resulted in the destruction, migration, and local deposition of slope surface soil.

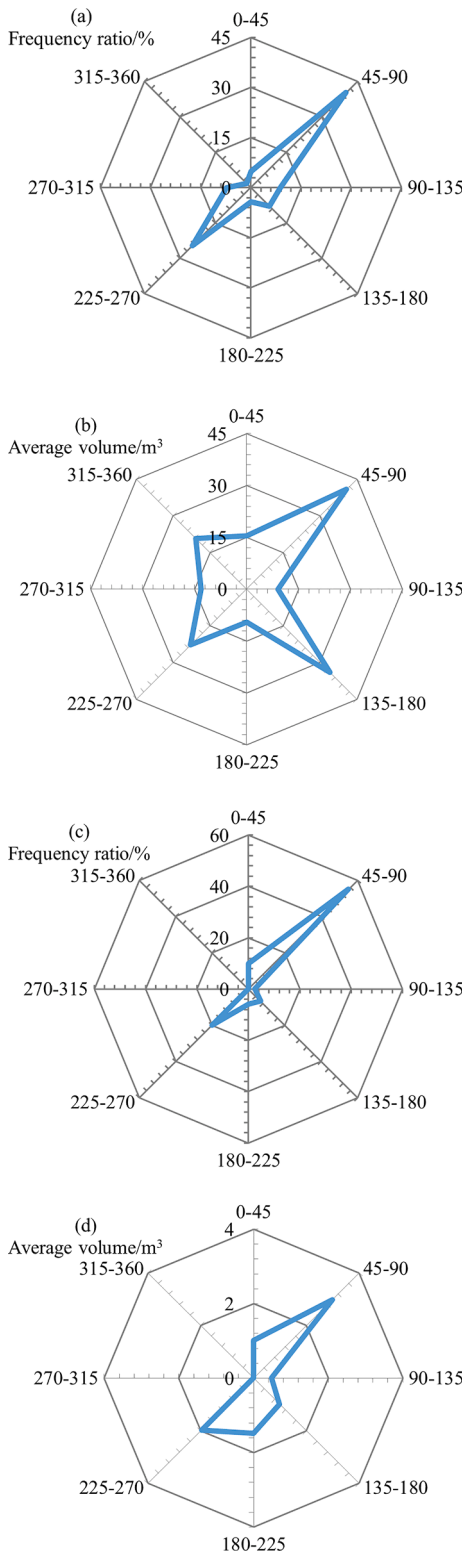

Fig. 4. The spatial distribution of artificial slope instability in the Gutun watershed: the frequency ratio (a) and average volume (b) of slope instability; the frequency ratio (c) and average volume (d) of platform instability.

Small erosion gully was gradually formed in the slope with the decline of soil shear strength (Teixeira Guerra et al., 2017). **2) Expanding deformation period.** Small ground subsidence and erosion gully would increase in the width and depth over time, which would gradually evolve into the penetrating sinkhole. The sinkhole provides the more convenient channel of rainfall infiltration and surface water infusion (Zhang and Li, 2011; Zhang et al., 2013). The rainfall staying in loess pores could lead to the increase of hydrostatic and hydrodynamic pressure in the slope, which would accelerate the dissolution of salt soluble material. The cohesion of soil particles further decreases under the chemical action resulting the decline of soil shear strength. Meanwhile, the self-weight of the slope would rise with the increase of slope's moisture, which cause the rising of the slope's sliding force. Under the long-term physical, mechanical and chemical actions, the risk of slope instability would increase gradually (Liang et al., 2018). **3) Instability failure period.** Internal soil shear strength would be completely dissolved with the gradually saturated slope loess. When the sliding force produced by gravitation was close to or greater than its friction force, the landslide, collapse, and slump will be triggered (Xu et al., 2012; Guzzetti et al., 2012). Therefore, various categories of artificial slope instability have internal relevance, small instability might develop into a geological hazard without taking effective measures to prevent it from happening.

4.2. *Instability distribution affected by soil moisture and failure mode*

The difference of soil moisture in varying slope aspects and positions was an important factor affecting instability distribution of artificial slope. Researchers founded that water is the power supply in forming slope instability, there would be no instability without water (Malamud et al., 2004; Peng et al., 2018). As is widely recognized, loess is sensitive to the change of soil moisture, and its shear strength decreases sharply with the increase of soil moisture (Zhang and Liu, 2010; Li. 2018). Thus, this study compared the soil moisture of 6 artificial slopes with 4 layers (3 sunny slopes and 3 shady slopes) to analyze whether soil moisture would affect the instability distribution. Soil moisture at the varying position of sunny slopes was lower than that of shady slopes, which might be related to weaker evapotranspiration effect in the shady slopes (Fig. 8). Higher soil moisture in the shady slopes caused lower soil shear strength, so the shady slopes were more vulnerable to failure and instability (Qiu et al., 2017; Peng et al., 2019). Meanwhile, soil moisture gradually increased from the top to toe, and the maximum occurred at the slope 4 and the platform 3. In general, soil moisture of lower slopes and platforms comes from the rainfall infiltration and surface runoff from the upper slopes. The superimposition effect led to the difference in soil moisture which affects the vertical distribution of the instabilities (Rupke et al., 2007). As a result, soil moisture difference had a significant effect on the distribution of artificial slope instability.

The different failure modes of varying slope positions in a slope also had a significant impact on the vertical distribution of the instability. A tremendous amount of rainfall infiltration was the main reason for the instability of the top slope (Tang et al., 2015). The ponding of natural slope flew to artificial slope through the surface runoff during the heavy rainfall, which caused some deformation with the rapid increase of soil moisture at the top slope. As the increase of soil weight and the decrease of soil shear strength, the slump gradually developed in the top slope with the nearly vertical gradient (Zhang and Li, 2011). The instability of the middle slope was related to serious soil erosion caused by the superposition effect of rainfall accumulation (Rupke et al., 2007). A large amount of surface runoff led to the formation of erosion gully in the slope, causing the expansion of gully size over time. Meanwhile, part of the runoff infiltrated along cracks, joints, and fissures to form pore water pressure and produced sliding force, which lead to instability in the middle slope (Zhou et al., 2014). The instability of the lower slope was significantly affected by the lateral erosion or manual excavation. The internal weak surface of the slope was exposed under the lateral erosion and manual excavation, and the slope was prone to instability due to the lack of support (Wang et al., 2014; Giordan et al., 2017). It is noteworthy that the risk of instability in the lower slopes and the platforms would increase if the instability has occurred in the upper slope.

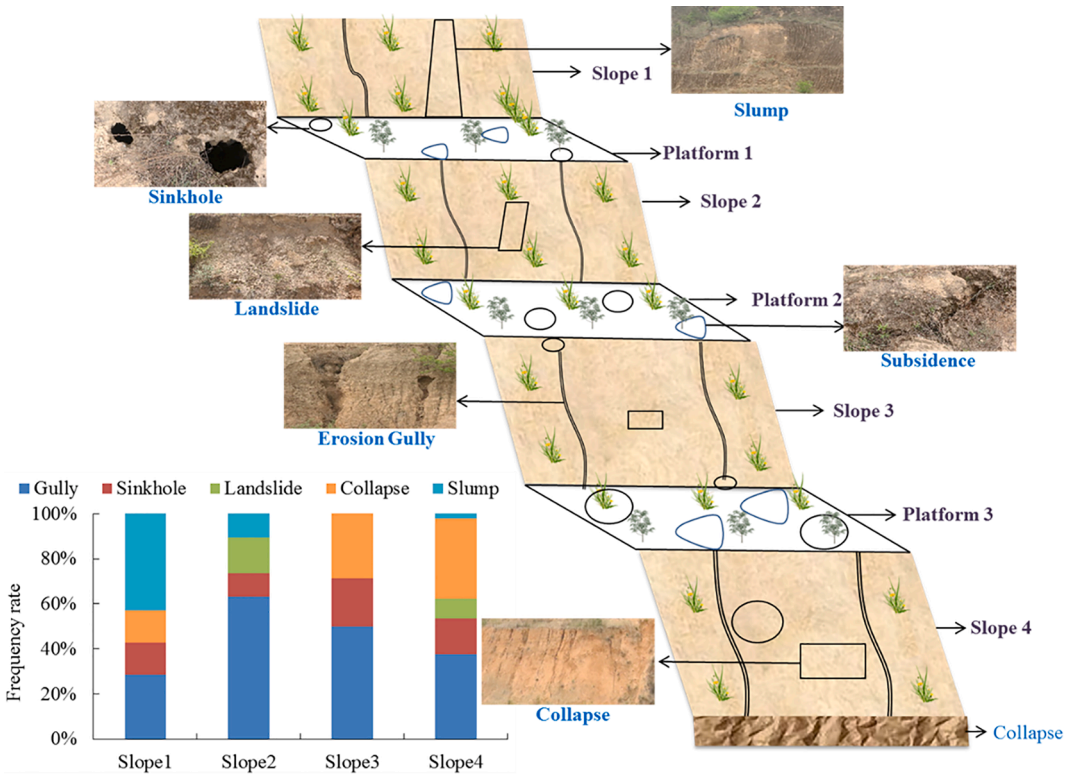

Fig. 5. The vertical distribution of artificial slope instability in the Gutun watershed.

4.3. *Different influencing degrees of surface condition factors*

The instability of artificial slope was triggered by external factors, while its size was greatly related to the surface condition factors of the slope. Our results showed that the volume of slope instability had a positive correlation with slope gradient and height, which was consistent with previous studies (Trigila et al., 2015; Zhang et al., 2021). Several researchers had found that a certain slope gradient and height are the necessary conditions for slope instability. Stress concentration at the toe of slope and erosion intensity of surface runoff would enhance with the increasing slope gradient and height based on numerical investigations and simulations (Frattini and Crosta, 2013; Zhuang et al., 2016; Qiu et al., 2018). The increase of stress would easily lead to the formation of tension zone and tensile crack at the top of the slope and platform, which cause cumulative instability process of artificial slope (Peng et al., 2016). With the increase of slope gradient and height, the speed of surface runoff would obviously enhance, which resulted in the erosion intensity of slope surface were significantly exacerbated and consequently led to the rising risk of slope instability. Meanwhile, due to the fact that vegetation is difficult to grow normally in the steep slopes, which resulted in the lack of effective vegetation protection of slope surface. Since the artificial slope gradient is usually large aiming for creating more farmland in the process of the GLCP, which increased the potential risk of slope instability (Ai et al., 2019).

This study also found that soil stability negatively impacted the instability volume of slope and platform. Soil compactness is an indication reflecting the soil ability to resist external forces, which has been widely applied in the instability evaluation of subgrade and slope of highway and railway. A higher soil compactness means a lower soil porosity, which could effectively reduce rainfall infiltration and improve erosion resistance (Imhoff et al., 2004; Somavilla et al., 2017). Soil shear strength refers to the ultimate strength of soil to resist shear failure. Previous research showed that most instabilities of loess slope could be ascribed to shear failure. Thus, the loess with higher soil shear strength is more difficult to be damaged under the external forces (Zhuang et al., 2018; Li, 2018). Meanwhile, there was no obvious connection between the volume of artificial slope instability and vegetation coverage in this study. This results might associate with no significantly different vegetation coverage among investigated artificial slopes, but the important role of vegetation coverage in slope stability shall not be ignored (Li et al., 2016; Zhang et al., 2019).

4.4. *Prevention mechanism of artificial slope instability*

Previous successful practices and research findings indicated that instability prevention of artificial slope after the GLCP should improve slope surface condition to reduce the infiltration and erosion of rainfall. However, traditional prevention measures of natural slope could not be completely copied due to the different geometry and stress structure of artificial slope. In addition, large-scale engineering measures, albeit are widely used in artificial slope on the sides of highway and railway, are not suitable because the GLCP aimed to coordinate ecological restoration and agricultural production (Liu et al., 2016; Liu and Li, 2017). To reduce the risk of artificial slope instability after the GLCP, we suggest adopting layered prevention and comprehensive measures according to its characteristics, distribution, and influencing factors. Hence, this study proposes a "Drain – Improve – Green - Reinforce (DIGR)" system from landscape coordination and structural stability as the prevention mechanism of artificial slope instability. The DIGR system is using various measures including the drainage system, soil improvement, vegetation protection and reinforcement engineering to realize the aims of "upper cut-off, lower block, and middle protection" (Fig. 9).

(a) **Drainage system.** A perfect interception and drainage facility is the most effective way to reduce infiltration and erosion of the rainfall. Long-term practices indicated interception drain could decrease surface runoff of the slope to minimize the erosion intensity (Zhou et al., 2014). Thus, the interception drain must be excavated along the slope edge at each platform, particularly at the top of slope. The depth and width of interception drain would

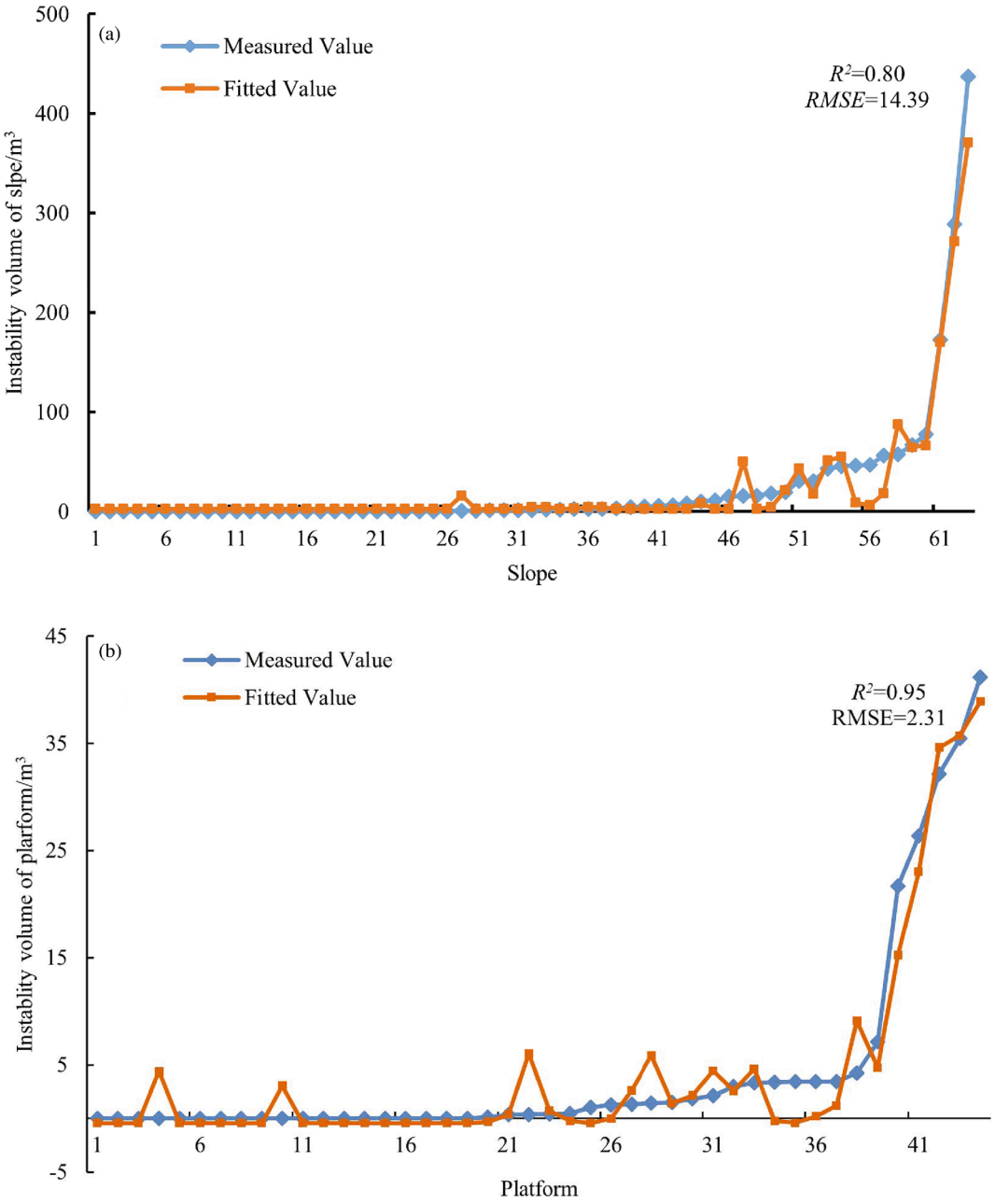

Fig. 6. The comparison results between fitted and measured values of the BPNN of slope (a) and platform (b) instability.

Table 2
The MIV of influencing factors of artificial slope instability.

	Factor	MIV		Factor	MIV
Slope Instability	Aspect	0.02	Platform Instability	Aspect	0.02
	Gradient	0.45		Width	0.05
	Height	0.12		Soil compactness-0 cm	−0.12
	Soil compactness-0 cm	−0.04		Soil compactness-10 cm	−0.16
	Soil compactness-10 cm	−0.14		Soil compactness-20 cm	−0.09
	Soil hear strength	−0.11		Soil shear strength	−0.06
	Arbor coverage	0.00		Arbor coverage	−0.01
	Shrub coverage	0.00		Shrub coverage	−0.01
	Grass coverage	0.01		Grass coverage	0.01
	Moss coverage	−0.01			

decide by the slope condition and catchment area, and its form could be high in the middle and low in the sides or high in the sides and low in the middle. The longitudinal drainage ditch must be arranged at the interception drain position on each slope, and its end should be connected with the channel at the toe of slope (Xu et al., 2012; Liu and Li, 2017; He et al., 2020).

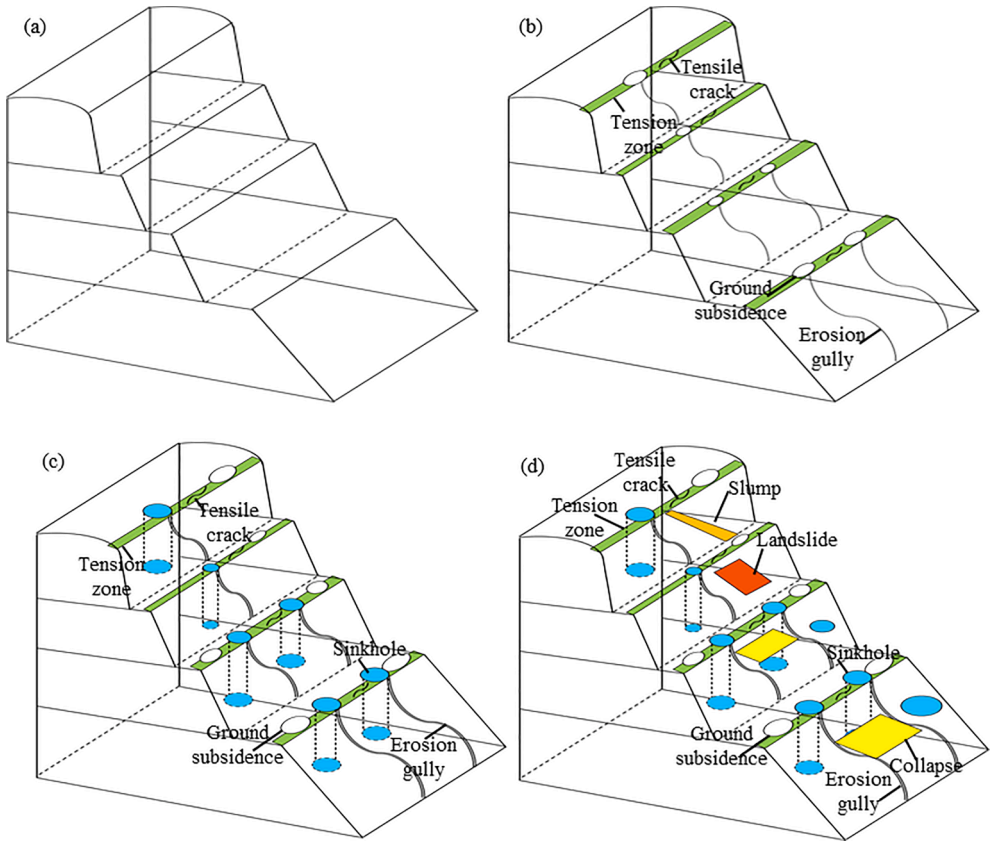

Fig. 7. The cumulative instability process of artificial slope: steady stage (a), creeping deformation stage (b), expanding deformation period (c) and instability failure period (d).

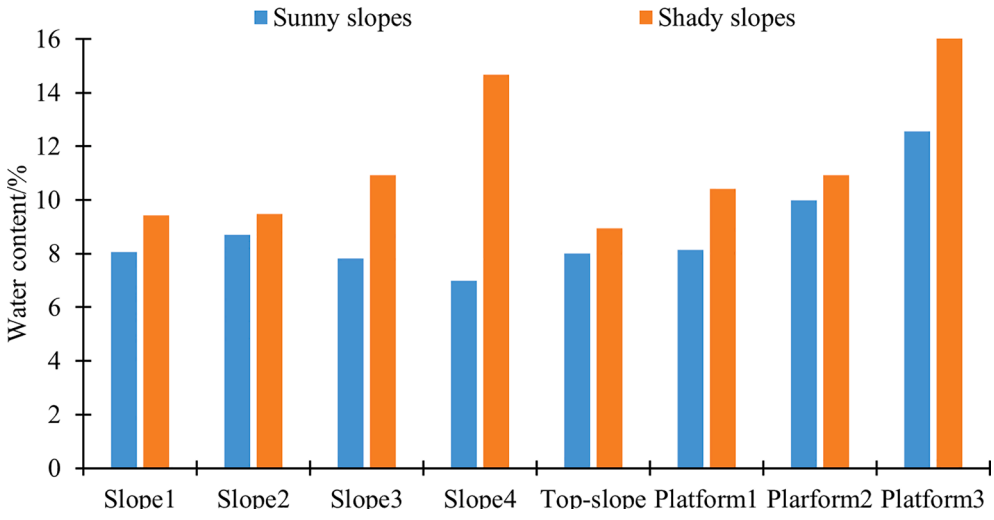

Fig. 8. The soil moisture of artificial slopes in the Gutun watershed.

(b) **Soil improvement.** The physical and chemical methods should be widely applied to improve soil structure and its shear strength for the decline of the instability risk of artificial slopes. Soil compaction is a physical method of enhancing soil strength in engineering construction, which could effectively reduce soil porosity and improve soil supporting force (Somavilla et al., 2017; Xia et al., 2019). Thus, the vibration compaction method should be adopted to conduct layered repeated compaction as the conditions permit in artificial slopes' excavation process. Meanwhile, several studies found that using soil stabilizer as a chemical method could achieve satisfactory results of soil improvement and slope protection (Stokes et al., 2010; Liu et al., 2019). We could select a soil stabilizer with economic, environmental, and effectiveness to spray or cover on the surface of artificial slopes. For example, Zhao et al. (2018) developed a soil stabilizer using thermally processed wood, bark fibers, and charcoal, which had achieved relatively good soil improvement and slope protection effect in Wuqi County of the LP.

(c) **Vegetation protection.** Field experiments showed that slope erosion and instability probability decrease with vegetation

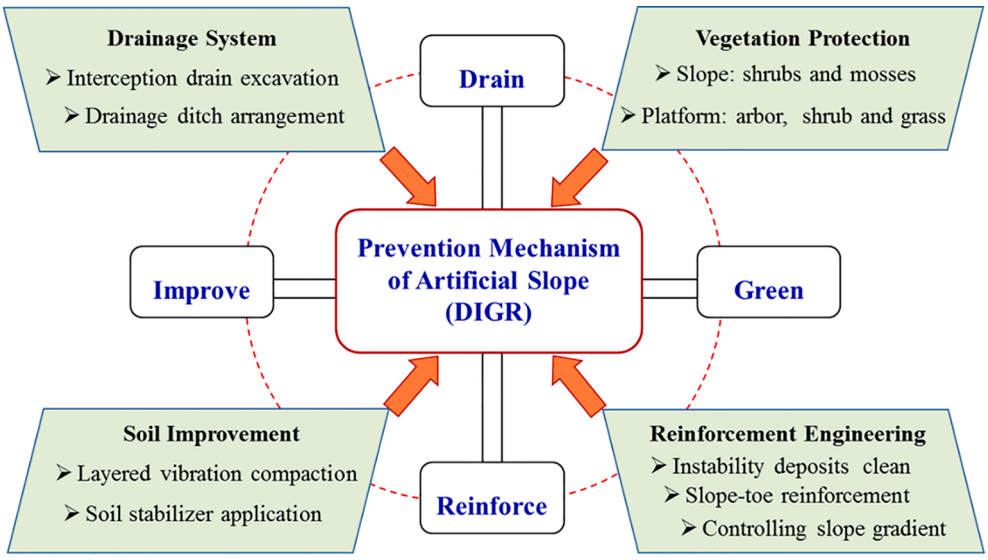

Fig. 9. The framework of prevention mechanism of artificial slope instability ("DIGR" system).

coverage and species richness (Wang et al., 2020). One reason is the interception function of the vegetation weakens the kinetic energy of raindrops and separates surface runoff (Zhang et al., 2019). Another explanation is soil compaction and its shear strength would be enhanced by coiling and consolidating of the roots (Li et al., 2016). Some studies also found that the shrub and moss were more effective than the arbor in slope protection, the reason of which is because of the destructive effect of arbor roots which might induce preferential flow to reduce soil ability (Xu et al., 2012). Hence, we recommend that moss and native species with fast growth, strong resistance and developed root could be planted to construct three-dimensional vegetation protection on the artificial slope. Each slope should be fully covered with the moss and shrub such as *Amorpha fruticosa* Linn. and *Vitex negundo* L. var. *heterophylla* (Franch.) Rehd.,. The single row of arbor (*Ailanthus altissima* (Mill.) *Swingle*, and *Robinia pseudoacacia* Linn.) and shrub (*Hippophae rhamnoides* Linn. and *Caragana korshinskii* Kom.) and the hole-sowing grass (*Zoysia japonica* Steud. and *Stipa bungeana* Trin.) should be planted alternately in each platform.

(d) **Reinforcement engineering.** Instability deposits should be cleaned timely in the upper slopes to prevent further instability in the lower slopes. For the slopes with severe instabilities or relatively larger height, the necessary engineering should be carried out at the toe of slope, such as constructing a retaining wall composed of coarse-grained materials, building dry stone stacking sandbags (Peng et al., 2019; Levett et al., 2020). Meanwhile, the slope gradient should be controlled between 45° to 65° and the height of each slope needs be contained in 4–6 m in future GLCP. The practice of neglecting the gradient and height of artificial slopes to increase the areas of new farmland should not be encouraged (Liu and Li, 2017; Feng et al., 2019).

5. Conclusions

Aiming at the artificial slope instability after the GLCP in the LP, this paper analyzed the characteristics and distribution of instability after the GLCP through a field investigation in the Gutun watershed. We further explored the impacts of surface condition factors on instability scale through BPNN method and proposed the prevention mechanism. Our results showed that artificial slope instability is a cumulative process induced by infiltration and erosion which causes various categories of instabilities. Instability degrees in shady slopes were higher than those in sunny slopes and gradually increased from top to toe in the vertical direction, which were closely related to the difference of soil moisture and failure mode. The volume of slope instability had a positive correlation with slope gradient and height, and soil compactness and shear strength negatively impacted the instability volume of slope and platform. The prevention mechanism of "Drain-Improve-Green-Reinforce (DIGR)" system was proposed to effectively reduce the risk of artificial slope instabilities after the GLCP. Compared with the previous studies, this paper focused on the artificial slope instability after land consolidation. The prevention mechanism of "DIGR" system is based on the ecology, economy, and effectiveness. However, more typical case studies are still needed to evaluate the stability of artificial slopes comprehensively. Also, monitoring, in-situ tests, and laboratory experiments are merited to shed light on the process and thresholds of the instabilities and the effects of the prevention mechanism.

Declaration of Competing Interest

The authors declare that they have no known competing financial interests or personal relationships that could have appeared to influence the work reported in this paper.

Acknowledgements

This study was funded by the National Key Research and Development Program of China (grant number 2017YFC0504701).

References

Acharya, G., Cochrane, T., Davies, T., Bowman, E., 2011. Quantifying and modeling post-failure sediment yields from laboratory-scale soil erosion and shallow landslide experiments with Silty Loess. Geomorphology 129(1-2), 49–58. https://doi.org/10.1016/j.geomorph.2011.01.012.

Ai, X., Sheng, M., Su, X., Ai, S., Jiang, X., Yang, S., Huang, Z., Ai, Y., 2019. Effects of frame beam on structural characteristics of artificial soil on railway cut-slopes in southwestern China. Land. Degrad. Dev. 32 (1), 482–493. https://doi.org/10.1002/ldr.v32.110.1002/ldr.3719.

Ai, X., Wang, L.i., Xu, D., Rong, J., Ai, S., Liu, S., Li, C., Ai, Y., 2021. Stability of artificial soil aggregates for cut slope restoration: A case study from the subalpine zone of Southwest China. Soil. Till. Res. 209, 104934. https://doi.org/10.1016/j.still.2021.104934.

Chen, S., Ai, X., Dong, T., Li, B., Luom, R., Ai, Y., Chen, Z., Li, C., 2016. The physico-chemical properties and structural characteristics of artificial soil for cut slope restoration in Southwestern China. Sci. Rep-UK 6 (20565), 2016. https://doi.org/10.1038/srep20565.

Chen, Y., Wang, K., Lin, Y., Shi, W., Song, Y.i., He, X., 2015. Balancing green and grain trade. Nat. Geosci. 8 (10), 739–741. https://doi.org/10.1038/ngeo2544.

Cho, S.E., Lee, S.R., 2001. Instability of unsaturated soil slopes due to infiltration. Comput. Geotech. 28 (3), 185–208. https://doi.org/10.1016/S0266-352X(00)00027-6.

Crozier, M.J., 1999. Prediction of rainfall-triggered landslides: A test of the antecedent water status model. Earth Surf. Proc. Land. 24 (9), 825–833. https://doi.org/10.1002/(SICI)1096-9837(199908)24:9<825::AID-ESP14>3.0.CO;2-M.

Derbyshire, E., 2001. Geological hazards in Loess Terrain, with particular reference to the Loess Regions of China. Earth-Sci. Rev. 54 (1), 231–260. https://doi.org/10.1016/S0012-8252(01)00050-2.

Erzin, Y., Cetin, T., 2012. The use of neural networks for the prediction of the critical factor of safety of an artificial slope subjected to earthquake forces. Sci. Iran. 19 (20), 188–194. https://doi.org/10.1016/j.scient.2012.02.008.

Erzin, Y., Nikoo, M., Nikoo, M., Cetin, T., 2016. The use of self-organizing feature map networks for the prediction of the critical factor of safety of an artificial slope. Neiral. Netw. World. 26 (5), 461–475. https://doi.org/10.14311/NNW.2016.26.027.

Feng, L.i., Zhang, M., Jin, Z., Zhang, S., Sun, P., Gu, T., Liu, X., Lin, H., An, Z., Peng, J., Guo, L.i., 2021. The genesis, development, and evolution of original vertical joints in Loess. Earth-Sci. Rev. 214, 103526. https://doi.org/10.1016/j.earscirev.2021.103526.

Feng, Weilun, Li, Yurui, 2021. Measuring the ecological safety effects of land use transitions promoted by land consolidation projects: the case of Yan'an City on the Loess Plateau of China. Land 10 (8), 783. https://doi.org/10.3390/land10080783.

Feng, W., Liu, Y., Chen, Z., Li, Y., Huang, Y., 2019. Theoretical and practical research into excavation slope protection for agricultural geographical engineering in the Loess Plateau: A case study of China's Yangjuangou Catchment. J. Rural Stud. DIO. https://doi.org/10.1016/j.jrurstud.2019.01.020.

Frattini, P., Crosta, G.B., 2013. The role of material properties and landscape morphology on landslide size distributions. Earth Planet. Sci. Lett. 361, 310–319. https://doi.org/10.1016/j.epsl.2012.10.029.

Garakani, A.A., Haeri, S.M., Khosravi, A., Habibagahi, G., 2015. Hydro-mechanical behavior of undisturbed collapsible Loessial soils under different stress state conditions. Eng. Geol. 195, 28–41. https://doi.org/10.1016/j.enggeo.2015.05.026.

Guzzetti, F., Carrara, A., Cardinali, M., Reichenbach, P., 1999. Landslide hazard evaluation: A review of current techniques and their application in A multi-scale study, Central Italy. Geomorphology 31 (1–4), 181–216. https://doi.org/10.1016/S0169-555X(99)00078-1.

Guzzetti, F., Mondini, A., Cardinali, M., Fiorucci, F., Santangelo, M., Chang, K., 2012. Landslide inventory maps: new tools for an old problem. Earth-Sci. Rev. 112 (1–2), 42–66. https://doi.org/10.1016/j.earscirev.2012.02.001.

Giordan, D., Cignetti, M., Baldo, M., Godone, D., 2017. Relationship between Man-Made Environment and Slope Stability: the Case of 2014 Rainfall Events in the Terraced Landscape of the Liguria Region (Northwestern Italy). Geomat. Nat. Haz. Risk 8 (1), 1833–1852. https://doi.org/10.1080/19475705.2017.1391129.

Gomez, H., Kavzoglu, T., 2005. Assessment of Shallow Landslide Susceptibility Using Artificial Neural Networks in Jabonosa River Basin. Venezuela. Eng. Geol. 78 (1), 11–27. https://doi.org/10.1016/j.enggeo.2004.10.004.

He, M., Wang, Y., Tong, Y., Zhao, Y., Qiang, X., Song, Y., Wang, L.i., Song, Y.i., Wang, G., He, C., 2020. Evaluation of the Environmental Effects of Intensive Land Consolidation: A Field-Based Case Study of the Chinese Loess Plateau. Land Use Policy 94, 104523. https://doi.org/10.1016/j.landusepol.2020.104523.

Jia, N., Mitani, Y., Xie, M., Tong, J., Yang, Z., 2015. GIS Deterministic Model-Based 3D Large-Scale Artificial Slope Stability Analysis Along a Highway Using a New Slope Unit Division Method. Nat. Hazards. 76 (2), 873–890. https://doi.org/10.1007/s11069-014-1524-6.

Jin, Z., Guo, L., Wang, Y., Yu, Y., Henry, L., Chen, Y., Chu, G., Zhang, J., Zhang, N., 2019. Valley Reshaping and Damming Induce Water Table Rise and Soil Salinization on the Chinese Loess Plateau. Geoderma. 339, 115–125. https://doi.org/10.1016/j.geoderma.2018.12.048.

Jin, Z., 2014. The Creation of Farmland by Gulling Filling on the Loess Plateau: a Double-Edge Sword. Environ. Sci. Technol. 48 (2), 883–884. https://doi.org/10.1021/es405392c.

Imhoff, S., Da Silva, A.P., Fallow, D., 2004. Susceptibility to Compaction, Load Support Capacity, and Soil Compressibility of Hapludox. Soil Sci. Soc. Am. J. 68 (1), 17–24. https://doi.org/10.2136/sssaj2004.1700.

Lee, J.-W., Park, C.-M., Rhee, H., 2013. Revegetation of Decomposed Granite Roadcuts in Korea: Developing Digger, Evaluating Cost Effectiveness, and Determining Dimensions of Drilling Holes, Revegetation Species, and Mulching Treatment. Land. Degrad. Dev. 24 (6), 591–604. https://doi.org/10.1002/ldr.2248.

Lee, T., Lin, H., Lu, Y., 2009. Assessment of Highway Slope Failure Using Neural Networks. J. Zhejiang University-Sci. A. 10 (1), 1010–1108. https://doi.org/10.1631/jzus.A0820265.

Levett, A., Gagen, E., Zhao, Y., Vasconcelos, P., Southam, G., 2020. Biocement stabilization of an experimental-scale artificial slope and the reformation of iron-rich crusts. Proc. Natl. Acad. Sci USA 117 (31), 18347–18354. https://doi.org/10.1073/pnas.2001740117.

Li, Y., 2018. A review of shear and tensile strengths of the Malan Loess in China. Ecol. Eng. 236, 4–10. https://doi.org/10.1016/j.enggeo.2017.02.023.

Li, Y., Li, Y., Fan, P., Long, H., 2019. Impacts of Land Consolidation on Rural Human-Environment System in Typical Watershed of the Loess Plateau and Implications for Rural Development Policy. Land Use Policy. 86, 339–350. https://doi.org/10.1016/j.landusepol.2019.04.026.

Li, Y., Wang, Y., Ma, C., Zhang, H., Wang, J., Song, S., Zhu, J., 2016. Influence of the Spatial Layout of Plant Roots on Slope Stability. Ecol. Eng. 91, 477–486. https://doi.org/10.1016/j.ecoleng.2016.02.026.

Li Y., Zhang X., Cao Z., Liu Y., Liu Z., 2021. Towards the Progress of Ecological Restoration and Economic Development in China's Loess Plateau and Strategy for More Sustainable Development. Sci. Tot. Environ. 756, 143676. https://doi.org/10.1016/j.scitotenv.2020.143676.

Liang, C., Cao, C., Wu, S., 2018. Hydraulic-Mechanical Properties of Loess and its Behavior When Subjected to Infiltration-Induced Wetting. Bull. Eng. Geol. Environ. 77 (1), 385–397. https://doi.org/10.1007/s10064-016-0943-x.

Liu, J., Chen, Z., Kanungo, D.P., Song, Z., Bai, Y., Wang, Y., Li, D., Qian, W., 2019. Topsoil Reinforcement of Sandy Slope for Preventing Erosion Using Water-Based Polyurethane Soil Stabilizer. Eng. Geol. 252, 125–135. https://doi.org/10.1016/j.enggeo.2019.03.003.

Liu, Yansui, Feng, Weilun, Li, Yurui, 2020. Modern agricultural geographical engineering and agricultural high-quality development: Case study of loess hilly and gully region. Acta Geographica Sinica 75 (10), 2029–2046. https://doi.org/10.11821/dlxb202010001.

Liu, Y., Li, Y., 2017. Engineering Philosophy and Design Scheme of Gully Land Consolidation in Loess Plateau. Trans. Chin. Soc. Agric. Eng. 33 (10), 1–9. https://doi.org/10.11975/j.issn.1002-6819.2017.10.001.

Liu, Yansui, Long, Hualou, Chen, Yufu, Wang, Jieyong, Li, Yurui, Li, Yuheng, Yang, Yuanyuan, Zhou, Yang, 2016. Progress of research on urban-rural transformation and rural development in China in the past decade and future prospects. Journal of Geographical Sciences 26 (8), 1117–1132. https://doi.org/10.1007/s11442-016-1318-8.

Liu, Yansui, Wang, Yongsheng, 2019. Rural land engineering and poverty alleviation: Lessons from typical regions in China. Journal of Geographical Sciences 29 (5), 643–657. https://doi.org/10.1007/s11442-019-1619-9.

Lukić, T., Bjelajac, D., Fitzsimmons, K.E., Marković, S.B., Basarin, B., Mlađan, D., Micić, T., Schaetzl, R.J., Gavrilov, M.B., Milanović, M., Sipos, G., Mezősi, G., Knežević-Lukić, N., Milinčić, M., Létal, A., Samardžić, I., 2018. Factors Triggering Landslide Occurrence on the Zemun Loess Plateau, Belgrade Area, Serbia. Environ. Earth Sci. 77 (13) https://doi.org/10.1007/s12665-018-7712-z.

Malamud, B.D., Turcotte, D.L., Guzzetti, F., Reichenbach, P., 2004. Landslide Inventories and Their Statistical Properties. Earth. Surf. Proc. Land. 29 (6), 687–711. https://doi.org/10.1002/(ISSN)1096-983710.1002/esp.v29:610.1002/esp.1064.

Mota, J.F., Sola, A.J., Jiménez-Sánchez, M.L., Pérez-García, F., Merlo, M.E., 2004. Gypsicolous Flora, Conservation and Restoration of Quarries in the Southeast of the Iberian Peninsula. Biodivers. Conserv. 13 (10), 1797–1808. https://doi.org/10.1023/B:BIOC.0000035866.59091.e5.

Peng, J., Sun, P., Igwe, O., Li, X., 2018. Loess Caves, a Special Kind of Geo-Hazard on Loess Plateau, Northwestern China. Eng. Geol. 236, 79–88. https://doi.org/10.1016/j.enggeo.2017.08.012.

Peng, J., Wang, S., Wang, Q., Zhuang, J., Huang, W., Zhu, X., Leng, Y., Ma, P., 2019. Distribution and Genetic Types of Loess Landslides in China. J. Asian Earth Sci. 170, 329–350. https://doi.org/10.1016/j.jseaes.2018.11.015.

Peng, J., Wu, D., Duan, Z., Tang, D., Cheng, Y., Che, W., Huang, W., Wang, Q., Zhuang, J., 2016. Disaster Characteristics and Destructive Mechanism of Typical Loess Landslide Cases Triggered by Human Engineering Activities. J. Southwest Jiaotong Univ. 51 (5), 971–980. https://doi.org/10.3969/j.issn.0258-2724.2016.05.021.

Qiu, H., Cui, P., Regmi, A.D., Hu, S., Wang, X., Zhang, Y., 2018. The Effects of Slope Length and Slope Gradient on the Size Distributions of Loess Slides: Field Observations and Simulations. Geomorphology 300, 69–76. https://doi.org/10.1016/j.geomorph.2017.10.020.

Qiu, H., Regmi, A.D., Cui, P., Hu, S., Wang, Y., He, Y., 2017. Slope Aspect Effects of Loess Slides and its Spatial Differentiation in Different Geomorphologic Types. Arab. J. Geosci. 10, 344. https://doi.org/10.1007/s12517-017-3135-5.

Rupke, J., Huisman, M., Kruse, H., 2007. Stability of Man-Made Slopes. Eng. Geol. 91 (1), 16–24. https://doi.org/10.1016/j.enggeo.2006.12.009.

Shin, Y., Choi, J., Quinteros, S., Svendsen, I., Lheureux, J., Seong, J., 2020. Evaluation and Monitoring of Slope Stability in Cold Region: Case Study of Man-Made Slope at Oysand. Norway. Appl. Sci-Basel. 10 (12), 4136. https://doi.org/10.3390/app10124136.

Somavilla, A., Gubiani, P.I., Reichert, J.M., Reinert, D.J., Zwirtes, A.L., 2017. Exploring the Correspondence between Precompression Stress and Soil Load Capacity in Soil Cores. Soil Till. Res. 169, 146–151. https://doi.org/10.1016/j.still.2017.02.003.

Stokes, A., Sotir, R., Chen, W., Chestem, M., 2010. Soil Bio- and Eco-Engineering in China: Past Experience and Future Priorities Preface. Eng. Geol. 36 (3), 247–257. https://doi.org/10.1016/j.ecoleng.2009.07.008.

Suman, S., Khan, S.Z., Das, S.K., Chand, S.K., 2016. Slope Stability Analysis Using Artificial Intelligence Techniques. Nat. Hazards 84 (2), 727–748. https://doi.org/10.1007/s11069-016-2454-2.

Sutejo, Y., Gofar, N., 2015. Effect of Area Development on the Stability of Cut Slopes. Procedia. Engineering. 125, 331–337. https://doi.org/10. 1016/j.proeng.2015.11.071.

Tan, Q., Bai, M., Zhou, P., Hu, J., Qin, X., 2021. Geological Hazard Risk Assessment of Line Landslide Based On Remotely Sensed Data and GIS. Measurement. 169, 108370. https://doi.org/10.1016/j.measurement.2020.108370.

Tang, Y., Xue, Q., Li, Z., Feng, W., 2015. Three Modes of Rainfall Infiltration Inducing Loess Landslide. Nat. Hazards 79 (1), 137–150. https://doi.org/10.1007/s11069-015-1833-4.

Teixeira Guerra, A.J., Fullen, M.A., Oliveira Jorge, M.D.C., Rodrigues Bezerra, J.F., Shokr, M.S., 2017. Slope Processes, Mass Movement and Soil Erosion: A Review. Pedosphere 27 (1), 27–41. https://doi.org/10.1016/S1002-0160(17)60294-7.

Trigila, A., Iadanza, C., Esposito, C., Scarascia-Mugnozza, G., 2015. Comparison of Logistic Regression and Random Forests Techniques for Shallow Landslide Susceptibility Assessment in Giampilieri (NE Sicily, Italy). Geomorphology 249, 119–136. https://doi.org/10.1016/j.geomorph.2015.06.001.

Tu, X.B., Kwong, A.K.L., Dai, F.C., Tham, L.G., Min, H., 2009. Field Monitoring of Rainfall Infiltration in a Loess Slope and Analysis of Failure Mechanism of Rainfall-Induced Landslides. Eng. Geol. 105 (1-2), 134–150. https://doi.org/10.1016/j.enggeo.2008.11.011.

Wang, H., Zhang, G., Li, N., Zhu, P., 2020. Variation in Soil Erosion Resistance of Slips Deposition Zone with Progressive Vegetation Succession on the Loess Plateau. China. J. Soil. Sediment. 20 (1), 234–248. https://doi.org/10.1007/s11368-019-02397-1.

Wang, J.-J., Liang, Y., Zhang, H.-P., Wu, Y., Lin, X., 2014. A Loess Landslide Induced by Excavation and Rainfall. Landslides 11 (1), 141–152. https://doi.org/10.1007/s10346-013-0418-0.

Wang, Y., Sun, H., Zhao, Y., 2019. Characterizing Spatial-Temporal Patterns and Abrupt Changes in Deep Soil Moisture across an Intensively Managed Watershed. Geoderma 341 (1), 181–194. https://doi.org/10.1016/j.geoderma.2019.01.044.

Xia, P., Hu, X.L., Wu, S.S., 2019. Slope Stability Analysis Based on Group Decision Theory and Fuzzy Comprehensive Evaluation. J. Earth Sci. 31(6), 1121-1132. https://doi.org/10.1007/s12583-020-1101-8.

Xu, H., Wang, Y., Song, G., 2012. Causes and Countermeasures to Prevent and Control Slope Landslide for Freeway: The Third Period of Jingcheng Freeway (Shayugou-City Boundary Section of Beijing). Science of Soil and Water Conservation 10(5), 84-89. https://doi.org/ 10.16843/j.sswc.2012.05.013.

Zhang, B.-J., Zhang, G.-H., Yang, H.-Y., Zhu, P.-Z., 2019. Temporal Variation in Soil Erosion Resistance of Steep Slopes Restored with Different Vegetation Communities on the Chinese Loess Plateau. Catena 182, 104170. https://doi.org/10.1016/j.catena.2019.104170.

Zhang, F., Wang, G., Kamai, T., Chen, W., Zhang, D., Yang, J., 2013. Undrained shear behavior of loess saturated with different concentrations of sodium chloride solution. Eng. Geol. 155, 69–79. https://doi.org/10.1016/j.enggeo.2012.12.018.

Zhang, F., Zhao, C., Lourenço, S.D.N., Dong, S., Jiang, Y., 2021. Factors affecting the soil-water retention curve of Chinese loess. Bull. Eng. Geol. Environ. 80 (1), 717–729. https://doi.org/10.1007/s10064-020-01959-9.

Zhang, M., Li, T., 2011. Triggering Factors and Forming Mechanism of Loess Landslides. J. Eng. Geol. 19, 530-540. https: CNKI:SUN:GCDZ.0.2011-04-015.

Zhang, M., Liu, J., 2010. Controlling Factors of Loess Landslides in Western China. Envir. Earth Sci. 59 (8), 1671–1680. https://doi.org/10.1007/s12665-009-0149-7.

Zhao, X., Li, Z., Robeson, M.D., Hu, J., Zhu, Q., 2018. Application of Erosion-resistant Fibers in the Recovery of Vegetation on Steep Slopes in the Loess Plateau of China. Catena 160, 233–241. https://doi.org/10.1016/j.catena.2017.09.021.

Zhou, Y., Tham, L., Yan, R., Xu, L., 2014. The Mechanism of Soil Failures Along Cracks Subjected to Water Infiltration. Comput. Geotech. 55, 330–341. https://doi.org/10.1016/j.compgeo.2013.09.009.

Zhuang, J., Peng, J., Wang, G., Javed, I., Wang, Y., Li, W., 2018. Distribution and Characteristics of Landslide in Loess Plateau: A Case Study in Shaanxi Province. Eng. Geol. 236, 89–96. https://doi.org/10.1016/j.enggeo.2017.03.001.

Zhuang, J., Peng, J., Xu, Y., Xu, Q., Zhu, X., Li, W., 2016. Assessment and Mapping of Slope Stability Based on Slope Units: A Case Study in Yan'an, China. J. Earth Syst. Sci. 125, 1439–1450. https://doi.org/10.1007/s12040-016-0741-7.